Hydrol. Earth Syst. Sci. Discuss., 8, 9797–9841, 2011
www.hydrol-earth-syst-sci-discuss.net/8/9797/2011/
doi:10.5194/hessd-8-9797-2011

Hydrology and
Earth System
Sciences
Discussions

In-situ evaluation of internal drainage in layered soils (Tukulu, Sepane and Swartland)

S. S. W. Mavimbela and L. D. van Rensburg

Department of Soil, Crop and Climate Sciences, University of the Free State, P.O. Box 339, Bloemfontein, 9300, South Africa

Received: 3 September 2011 – Accepted: 23 October 2011 – Published: 8 November 2011

Correspondence to: S. S. W. Mavimbela (sabelomavimbela@yahoo.com)

Published by Copernicus Publications on behalf of the European Geosciences Union.

Abstract

The soil water release (SWC) and permeability properties of layered soils following deep infiltration depends on the structural and layering composition of the profiles diagnostic horizons. Three layered soils, the Tukulu, Sepane and Swartland soil forms, from the Free State province of South Africa, were selected for internal drainage evaluation. The soil water release curves as a function of suction (h) and unsaturated hydraulic conductivity (K-coefficient) as a function of soil water content, SWC (θ), were characterised alongside the pedological properties of the profiles. The water hanging column in collaboration with the in-situ instantaneous profile method (IPM) was appropriate for this work. Independently, the saturated hydraulic conductivity (K_s) was measured using double ring infiltrometers. The three soils had a generic orthic *A* horizon but differed remarkable with depth. A clay rich layer was found in the Tukulu and Sepane at depths of 600 to 850 mm and 300 to 900 mm, respectively. The Swartland was weakly developed with a saprolite rock found at depth of 400–700 mm. During the 1200 h drainage period, soil water loss amounted to 21, 20 and 51 mm from the respective Tukulu, Sepane and Swartland profiles. An abrupt drop in K_s in conjunction with a steep K-coefficient gradient with depth was observed from the Tukulu and Sepane. Hydromorphic colours found on the clay-rich horizons suggested a wet soil water regime that implied restriction of internal drainage. It was therefore concluded that the clay rich horizons gave the Tukulu and Sepane soil types restricted internal drainage properties required for soil water storage under infield rainwater harvesting production technique. The coarseness of the Swartland promoted high drainage losses that proliferated a dry soil water regime.

1 Introduction

Internal drainage has become a critical factor in soil water conservation especially on layered soils. Since the large soil pores are the first to drain following deep infiltration, their soil water release (SWR) and permeability is dependent on the structural and layering composition of the profiles diagnostic horizons. The SWR and permeability functions could be described by the SWR curve or soil water characteristic curve (SWCC) and unsaturated hydraulic conductivity (K-coefficient), respectively. While the former is expressed as a function of matrix suction (h) and SWC (θ) (Dane and Hopmans, 2002) the latter is expressed as a function of either h or θ (Eching and Hopmans, 1993).

In practice internal drainage depicts the emptying of water filled pores under the influence of gravity. In time and space, drainage rate diminishes with SWC approaching negligible levels once the drainage upper limit (DUL) has been realised at about 0.1 to 0.2 % per day (Ratliff et al., 1983). The DUL could further be reduced to approach the drainage lower limit (DLL), equivalent to the permanent wilting point (Hillel, 2004), by evaporation or transpiration (Bennie et al., 1994). In most vertical soils DUL could be achieved between 2 to 12 days for fine-textured soils and up to 20 days in soils with a restrictive layer (Ratliff et al., 1983). The difference between DUL and DLL represents the plant available water (PAW) that is important for estimating crop water requirements (Bennie et al., 1994; Bittelli and Flury, 2006). Therefore accurate measurement of the soil hydraulic functions that determines the extent at which soil water drains away from the profile is crucial for effective soil water management.

In situ internal drainage methods of determining soil hydraulic functions are considered to be more realistic than laboratory methods. Continuum of soil horizons represents the actual boundary conditions under which water flows in a composite profile. Internal drainage under in-situ conditions was first studied by Richard et al. (1956). Difficulties in measurement of K-coefficient under in-situ conditions because of variations in humidity and the need for simultaneous measurement of many parameters, transient experiments were preferred from the beginning. Early contributions included work by of Nielsen et al. (1964), Rose et al. (1965) and Watson (1966) that culminated to the launching of the instantaneous profile method (IPM) (Hopmans et al., 2002). Inversion of the Richard flow equation provided means to estimate the K-coefficient (Vachaud and Dane, 2002) indirectly from the ratio of drainage flux and effective hydraulic gradient. Other in-situ methods are the internal drainage and zero flux plane methods described by Vachaud et al. (1978) and tension disk infiltrometers (Hopmans et al., 2002; Simunek et al., 1999). The IPM was consolidated when the in-situ procedure to calculate the K-coefficient was published by Hillel et al. (1972). Among earlier studies the unity gradient become popular but was later disputed by Richardts (1993); Bacchi and Richardts (1993). To keep pace with the advances in the laboratory methods such as the one step (Kool et al., 1985) and multi-step (van Dam et al., 1994; Eching et al., 1994) outflow experiments, the IPM went through a series of modernization. This included the computational contributions by Libardi et al. (1980) and Bacchi (1988), and the parameterization of the Richard inversion by Richardts et al. (2004). The first to use parameters based models to inversely estimate soil hydraulic functions from in-situ experimental data was Dane and Hruska (1983), even though lack of uniqueness of their solution was a concern. Hurtado et al. (2005) used the IPM to estimate hydraulic functions below the DUL while Neto et al. (2007) introduced computer based software to calculate the K-coefficient in internal drainage experiments.

Despite the remarkable works done to improve in-situ internal drainage methods, laboratory transient experiments are still by far dominant. Better control of conditions and parameters influencing soil hydraulic functions as well as access to dynamic instrumentation and powerful computers has made laboratory experiments attractive. Transferring some of these technologies to developing farming communities has not been successful in many occasions. Nevertheless, approaches such as the pedo-transfer (Leij et al., 1996; Acutis and Donatelli, 2003) and hanging water column technique (Vomicil, 1965; Dane and Hopmans, 2002) if used in collaboration with the IPM could serve as relatively cheap and yet powerful alternatives.

In the Free State province of South Africa, most of the rural farmers are concentrated on the low agricultural potential areas predominated by layered soils. This group of soils belong to the Duplex land type (Soil Classification Working Group, 1991) and occupy more than 10 % of the provincial landscape (Hensley et al., 2006). Erratic soil water regimes common among this soils has led to the development of infield rainwater harvesting (IRWH) production technique (Hensley, 2000; FAO, 2009). This technique seeks to turnaround the high surface runoff and evaporation losses from the 550 mm annual rainfall associated with these soils into deep infiltration and soil water storage. However, the occurrence of clay rich layer either in the *B* or *C* horizon among this group of soils suggests that their conservational prospects for IRWH is dependent on the horizons physical characteristics and layering formation. On this account, the Tukulu, Sepane and Swarland soil forms (Soil Classification Working Group, 1991) were selected as representatives of these soils and the following objectives were pursuit: firstly, to describe the pedological properties that relate to the presence of layering on the three soil types. Secondly, to determine the soil water release, unsaturated hydraulic conductivity and drainage-time functions that characterised the internal drainage outcomes of layered soils.

2 Material and methods

2.1 Site location and soil classification

The field experiments were carried out at Paradys Experimental Farm (29°13′2″ S, 26°12′ E, altitude 1422 m) of the University of the Free State. Three sites were selected with different soil types to include a typical Swartland (Sw), Sepane (Se), and Tukulu (Tu) soil form, according to the Soil Classification Working Group (1991). Three soil profile pits were prepared in each site at distance intervals of 50 m. Each profile pit was excavated in a step-wise downward fashion to allow double ring infiltrometers for the determination of steady state or saturated hydraulic conductivity for individual horizons. Soil samples from each horizon from these pits were taken for textural analysis and dry bulk density determination. Samples were oven dried at 105 °C for 24 h and particle size distribution was established using the pipette procedures proposed by the Non Affiliated Soil Analysis Work Committee (1990).

2.2 In-situ experimental set up and measurements

2.2.1 Saturated hydraulic conductivity

Saturated hydraulic conductivity (K_s) for the individual profile layers of the three soil types was measured using double ring infiltrometers as described by Scotter et al. (1982). On each excavated soil profile horizon both rings with diameters of 400 and 600 mm were fitted into the surface to a depth of 20 mm. A floater with 10 mm calibrated depths was inserted in the central position of the inner ring. The outside ring was first wetted and kept ponded through the experiment to prevent lateral flows. Then the inner ring was ponded immediately over some plastic material to prevent erosion of the surface until the depth of water settled to a calibrated mark on the floater. The clock timer was set and further changes in depths along the calibrated floater were recorded until a steady time was clocked by the falling water head. The saturated hydraulic conductivity (K_s, mm h^{-1}) was obtained by the falling head method described of Jury et al. (1991);

$$K_s = \frac{L}{t_1} \ln \frac{b_0 + L}{b_1 + L} \tag{1}$$

where L is the depth of the soil layer in question (mm), b_0 is the initial depth of total head above the soil column, b_1 is the depth that the falling head is not allowed to fall below (mm), t_1 is the time taken for b_0 to fall to b_1 (in hours). Once the steady state condition was established it was assumed that the soil matrix suction was negligible and did not affect macro-pore domain (Zavattaro and Grignani, 2001).

2.2.2 Instantaneous soil water measurement

A field representative site from each soil type was selected for the setting up of the in situ instantaneous profile method (IPM). The IPM provides a more realistic approach in capturing the flow dynamics in a heterogeneous soil profile subjected to variable hydraulic processes such as internal drainage and evaporation (Hopmans et al., 2002).

In the Sepane and Tukulu a more central position was selected and monoliths of (4 m × 4 m) × 1 m depth were prepared with three connected replications. Monoliths were centrally fitted with three neutron access tubes to a depth of 1.1 m. On the Swartland, the monoliths were detached and setup at 30 m distance apart with dimensions of (1.2 m × 1.2 m) × 0.5 m depth. Shallow depths on the Swartland allowed the use of DFM probe loggers at depths of 0.6 m. All monoliths were laterally isolated with plastic sheet to prevent lateral water movement. An earth bund was made to form a ridge around the monoliths to isolate them from surface runoff and to support ponding.

Before soil water content (SWC) measurements commenced the monoliths were ponded with water for three days until it was presumed to have reached field saturation. At the end of the 3rd day the monoliths were covered and sealed at the surface with a polythene plastic upon depletion of ponded water. Measurements of SWC were taken using a neutron water probe (NWP) at 200, 500, 850 and 1100 mm depth intervals. DFM probe loggers were set to take readings at every hour during the entire drainage period at depths of 100, 300 and 550 mm from the Swartland soil profile. Over the first seven days SWC measurements were taken in the morning and afternoon and thereafter once a day for a 50 day period. The measured SWC that resulted in a drainage flux of 0.001 mm h^{-1} was assumed to have reached the drainage upper limit (DUL). At the beginning of the field measurements both soil water instruments were calibrated for the respective soil profiles. From each horizon a soil sample was taken using an auger at a 250 mm distance from the NWP and DFM probe. Samples were weighed shortly after packaging in paper bags. They were then oven dried at 105 °C for 24 h to obtain gravimetric water content from their in-situ bulk densities.

2.3 Laboratory experimental setup and measurements

Undisturbed soil core samples were taken from the centre of each horizon using a core sampler mounted on a hydraulic jack. Samples were then trimmed, sealed and transported to the laboratory for analysis of the soil water characteristics curve (SWCC). Sampling cores had an inner diameter of 103 mm with a height of 77 mm.

Preparation of samples and desorption experiment was carried out in two phases. Core samples and water used for saturation samples were initially de-aired using a vacuum chamber pump set at −70 kPa for 48 h under room temperature. Subsequently, de-aired water was introduced on the second chamber with de-aired core samples allowing the inflow to wet samples from below. Ponded water outside the wetted sample was cut-off before water level overtopped the core samples. Core samples were left on the water bath for 24 h to allow total saturation. Three replications were used for each horizon. Before commencement of the desorption experiment saturated samples were weighed and sealed to control evaporation.

Although the desorption experiment involved three phases from 0–10 kPa, 10–100 kPa and 100–1500 kPa, in this work only the first was illustrated to capture the SWCC during internal drainage. This procedure involved the hanging soil water column tension cup method described by Dirksen (1999) and Dane and Hopmans (2002). Following saturation the samples were weighted and water that dripped from the sample at weighing time was attributed to the porosity of the samples. Placed on ceramic cups prepared for this purpose hanging 1000 mm from reference point samples, elevation height was gradually reduced at 100 mm intervals for the entire 1000 mm. At every step, interval samples were weighed before and after samples had equilibrated on the ceramic cups. During this experiment samples were covered with a foliar sheath to protect them from radiation. Considering that evaporation was assumed to be negligible under these conditions, change in samples mass was considered to be a true reflection of the amount of water that drained from the samples. The resulting suction-SWC (θ-h) relationship was then regressed to estimate the corresponding θ-h relationship to internal drainage of soil profiles horizons from saturation to drainage upper limit (DUL).

2.4 Data analysis

2.4.1 Estimation of unsaturated hydraulic conductivity

The unsaturated hydraulic conductivity (K-coefficient) was calculated using the IPM procedure as described by Sławiński et al. (2004) and Neto et al. (2007). One dimensional flux was computed using the mathematical expression:

$$q(z,t) = \int_{z=z_0}^{z} \frac{\partial\theta(z,t)}{\partial t} dz \tag{2}$$

where q is the flux (mm h^{-1}), θ is volumetric soil water content (mm mm^{-1}), t is the time in hours and z is the reference depth (mm).

The flux expression was then fitted to the extended Darcian law to express the K-coefficient as a function of SWC (θ);

$$K(\theta)(z,t) = \frac{\int_{z=z_0}^{z} \frac{\partial\theta(z,t)}{\partial t} dz}{\left(\frac{\partial h(z,t)}{\partial z} + 1\right)} \tag{3}$$

where $K(\theta)$ is the K-coefficient (mm h^{-1}), h is the matrix suction (mm) and t as defined in Eq. (2). The classical exponential equation proposed by Hillel et al. (1972) was used to obtain a linear regression function on the semi log scale for the plotted K-θ relationships.

2.4.2 Statistical analysis

The exponential function describing the K-θ relationships for the three soils were converted into a semi-log scale after which a linear regression coefficient and intercept for each horizon was determined. The coefficient of determination (R^2) provided the accuracy of the fit on the resulting semi-log linearized function. The linearized K-θ relationships were then evaluated for homogeneity using the Bartlett's test or chi-square (χ^2) distribution and pooled regression coefficient F-test as described by Gomez and Gomez (1984). Also the student's t-test was conducted to compare the regression coefficients between horizons within the same soil profile. Computed values were compared with Tabular values, which serve as bench marks at 95 % confidence intervals. If the former was found to be larger than the latter the homogeneity hypothesis was rejected.

3 Results

3.1 Pedological properties

Table 1 summarizes the physical and chemical properties of the Tukulu, Sepane and Swartland soils according to the *A*, *B* and *C* horizon layers. The results are also supported by soil profile photos in Figs. 1–3. Further reference is made to the profile descriptions in Tables A1–A3. All three soil types occurred within an area of less than 10 ha, on a straight mid slope of less than 1 %. However, both the Tukulu and Swartland occupied the upslope position with the former occurring along the smooth drainage lines. The Sepane soil form occupied most of the down slope areas of the experimental site. Although all the soil types had a generic orthic *A* horizon but differentiation in the *B* and *C* horizons gave each soil type unique layering properties.

Tukulu: The soil was classed as an orthic *A*-, neocutanic *B*- and prismatic *C* horizon. The clay plus silt fraction for the three horizons was 18 %, 31 % and 57 %, respectively with corresponding bulk density of 1670, 1597 and 1602 kg m^{-3}. Along with the increase in clay plus silt content with depth was the transformation in textural classes from fine sandy loam in the *A* horizon to a fine sandy clay loam in the *B* horizon and to clay in the *C* horizon. Corresponding horizons structural representations were the massive apedal of weakly sub angular blocky and moderate to strong prismacutanic structure, respectively. A smooth transition between the *A* and *B* horizons confirmed the common attributes of these horizons including among others colour, texture and youthfulness of structure. In contrast, the clear abrupt transition between the *B* and *C* horizon explained the sudden increase in clay plus silt in the *C* horizon, which gave the horizon grey colours compared to the red colours of the upper horizons. The distinct layering on the lower strata was also confirmed the sudden drop in K_s from 40 mm h^{-1} in the *B* horizon to 9.6 mm h^{-1} in the *C* horizon. Yellow, grey and olive mottled colours in the *C* horizon shown in Fig. 1b could also be regarded as indicators, not only of the intensity of layering, but also of the wet soil water regime of this horizon.

Sepane: The soil was classed as an orthic *A*, pedocutanic *B* and prismacutanic *C* horizon shown in Fig. 2. The clay plus silt fraction of the three horizons was 21 %, 41 % and 47 %, respectively. Corresponding bulk densities to the respective horizons were 1670, 1790 and 1730 kg m^{-3}. Accompanying the increase in clay plus silt content with depth, was the transformation in horizon textural classes from fine sandy loam in the *A* horizon to a fine sandy clay loam in the *B* horizon and to fine sandy clay in the *C* horizon. Structural properties unique to these horizon layers were the massive apedal, moderate to course sub angular blocky, and medium to strong prismatic structure, respectively. An abrupt transition between the *A* and *B* horizons and the smooth transition between the *B* and *C* horizons explained the concentration of structure between lower horizons of this soil. Changes in red colours from the surface to dull red and darker colours of the interior also pointed to layering that occurred at 300 mm depth splitting this soil into a weakly developed surface and well structured *B* and *C* horizons. Confirming the contrast in structure between the surface and *B* horizon were the well-developed and distinct peds with clay skins shown in Fig. 2b.

Swartland: The soil was classed as an orthic *A*, pedocutanic *B* and saprolite *C* horizon, shown in Fig. 3. The clay plus silt fraction for the three horizons was 14 %, 27 % and 21 %, respectively. Corresponding bulk densities to the respective horizons were 1670, 1530 and 1450 kg m^{-3}, respectively. A smooth transition occurred between the surface and *B* horizons indicating a gradual build-up in clay content, which resulted from the fine sandy loam in the *A* horizon transformed into a fine sandy clay loam in the *B* horizon. Between lower horizons there was an abrupt transition from a sub-angular blocky structure in the *B* horizon to the saprolite rock of the *C* horizon. The presence of dolorite intrusions and many black sesquioxides concretions shown in Fig. 3b at depths of 200–400 mm explained the general course appearance and lack of abrupt transition in this soil. Although levels of calcium and magnesium showed to increase with depth the predominance of a weakly weathered saprolite at shallow depths of 400 mm also reflected the deficiencies in structure and subsequent dry water regime of this soil.

3.2 θ-h relationship of soil horizons

Figure 4a–c shows the resulting θ-h relationships from the hanging column laboratory desorption of the Tukulu, Sepane and Swartland soil, respectively. Linear regression functions for each of the three soils horizons with the goodness of fit are shown in Table 2. Corresponding student's t-test analysis for differences between the horizons regressions coefficients are also presented in Table 3. Designated to capture the soil water release behaviour under internal drainage conditions, the θ-h relationship was set between the suction ranges of 0 to 1000 mm (10-kPa). Spatial variations among the three soils appeared to increase with suction, an essential indicator for evaluating the permissibility of water release by the various soil horizons.

Tukulu: The θ-h relationships from the *A*, *B* and *C* horizons appeared to cluster together at near zero suctions but after suctions of 200 mm their spatiality increased. The *A* horizon released water from 0.33 to 0.277 mm mm^{-1} while the *B* horizon showed a release from 0.325 to 0.285 mm mm^{-1} when suction was increased from 0 to 1000 mm. On the other hand, the *C* horizon released water from 0.324 to 0.321 mm mm^{-1} for the same suction range, resulting in a θ-h line that had an almost level slope. Effective saturation satisfied porosity only in the *C* horizon while the *A* and *B* horizons were below with 3 % and 1 %, respectively. Corresponding slopes to these θ-h relationships was 0.005 %, 0.004 % and 0.0003 % for the respective *A*, *B* and *C* horizons with the *B* horizon having the slowest water release function. Although the *A* and *B* horizon lines could be observed to be close to each other for the given suction range, the student's *t*-test captured no similarities. Linear regression functions fitted well the measured data with the R^2 of not less than 93 %.

Sepane: The *θ*-*h* relationships from the *A*, *B* and *C* horizons represented soil columns that exhibited different soil water release properties for the suction range in question. The *A* horizon released water from 0.328 to 0.257 mm mm^{-1} while the *B* horizon released from 0.332 to 0.289 mm mm^{-1} when suction was increased from 0 to 1000 mm. Similar to the *B* horizon was the *C* horizon that released water from 0.338 to 0.299 mm mm^{-1}. Effective porosity was 3.5 % and 1 % below porosity on the respective *A* and *B* horizons while in the *C* horizon the effective porosity was fairly satisfied. The resulting slopes from these *θ*-*h* relationships were 0.007 %, 0.004 % and 0.004 % for the *A*, *B* and *C* horizons, respectively. Interestingly, all three horizons *θ*-*h* functions had a goodness of fit not less than 99 %. Student's *t*-test also captured that the regression coefficients from these horizons were different.

Swartland: Variations in the *θ*-*h* relationships of all three soil horizons indicated a high permissible soil water release for the suction range in question. For suctions 0 to 1000 mm, the *A*, *B* and *C* horizons released water from 0.343 to 0.255 mm mm^{-1}, 0.348 to 0.287 mm mm^{-1} and 0.355 to 0.227 mm mm^{-1}, respectively. Effective saturation was 2 %, 12.8 % and 14.7 % below porosity from the respective *A*, *B* and *C* horizons. The *A*-horizon soil water release function had a slope of 0.008 % while the *B* horizon resembled a slope of 0.005 %. The greatest slope was found in the saprolite *C* horizon of about 0.012 %. When compared, regression coefficients from individual horizons *θ*-*h* functions were significantly different.

3.3 *K*-*θ* relationships of soil horizons

Resulting *K*-*θ* relationships from the in-situ desorption of *A*, *B* and *C* horizons of the Tukulu, Sepane and Swartland soils under internal conditions are shown in Fig. 5a–c, respectively. Corresponding regression exponential *K*-*θ* functions are presented in Table 4. Statistical homogeneity analysis is also illustrated in Tables 5 and 6. The differences in soils K-θ relationships reflected the spatial responses of drainage to the heterogeneity of soil layers permeability.

- Tukulu: the resulting K-θ relationships from the A, B and C horizons occupied the SWC range between 0.29 to 0.328 mm mm^{-1}. The K-θ lines of the A and B horizons were close to each other and were found in the interior, while that of the C horizon was exterior. The A horizon had K-θ coefficients ranging from 36.1 to 0.0005 mm h^{-1} for a SWC ranging of 0.328 to 0.297 mm mm^{-1}. The B horizon K-θ coefficient ranged from 40 to 0.0009 mm h^{-1} with a soil water range of 0.325 to 0.299 mm mm^{-1}. For the C horizon the K-θ coefficient ranged from 9.6 to 0.0005 mm h^{-1} for a drop in soil water content from 0.324 to 0.309 mm mm^{-1}. The K-θ relationships regression functions had R^2 of not less than 0.94 with the Bartletts test horizons were significantly different. However, the student's t-test found that K-θ relationships between A and B horizons were not comparable.

- Sepane: the resulting K-θ relationships from the A, B and C horizons occupied the SWC range between 0.292 to 0.338 mm mm^{-1}. The K-θ relationship of the A horizon inclined towards the interior while the B and C horizons were closer to each other and to the exterior. The A horizon had the K-θ coefficient ranging from 35.2 to 0.0007 mm h^{-1} for a soil water content ranging of 0.326 to 0.292 mm mm^{-1}. The B and C horizon K-θ coefficient dropped, respectively from 18.1 to 0.0015 mm h^{-1} and 1.9 mm h^{-1} to 0.0005 mm h^{-1} with a corresponding soil water content ranging from 0.332 to 0.316 mm mm^{-1} and 0.338 to 0.321 mm mm^{-1}. Bartletts homogeneity and pooled regression coefficient F-tests indicated that the K-θ relationships of this soil could not be described by one regression coefficient. However, the clay rich B and C horizons were not significantly different as determined by the student's t-test.

- Swartland: the resulting K-θ relationships from the A, B and C horizons occupied the SWC range between 0.22 to 0.344 mm mm^{-1}. The K-θ lines of the A and B horizons were close to each other and found on the exterior while that of the

C horizon was on the interior. The A-horizon showed a K-θ coefficient ranging from 23.5 to 0.0002 mm h^{-1} for a soil water content of 0.34 to 0.29 mm mm^{-1}. The K-θ coefficient for the B horizon ranged from 42.8 to 0.0007 mm h^{-1} with a SWC ranging from 0.344 to 0.299 mm mm^{-1}. For the C horizon the K-θ coefficient ranged from 76.5 to 0.001 mm h^{-1} with a soil water content ranging from 0.33 to 0.22 mm mm^{-1}. The K-θ relationships from the three horizons attained a goodness of fit of not less than 0.89. Failure of the Bartletts test of homogeneity was re-affirmed by the significant differences found by both the pooled regression coefficient F-test and student's t-test analyses. A different result was captured by the student's t-test when a comparison between the A and B horizon was made.

3.4 θ-T relationship of soil horizons

The θ-T relationship for the Tukulu, Sepane and Swartland soil types for the first 200 h of internal drainage are presented in Fig. 6. The power regression functions for the A, B and C horizons for these soils are presented in Table 7 and the student's t-test for the comparison of regression coefficients between horizons θ-T functions presented in Table 8. The presence of restrictive horizon layers influenced the manner in which these soils drained.

- Tukulu: the θ-T relationship for this soil indicated an increase in SWC with depth although each layer continued to drain instantaneously. The amount of water that drained away within the first 3 h was 5.1 mm from the orthic A and 2.4 mm from the neocutanic B horizon from an initial field saturation of 0.328 and 0.325 mm mm^{-1}, respectively. At field saturation of 0.324 mm mm^{-1} the C horizon lost 1.5 mm for the same period. At the end of the 200 h drainage period the A, B and C horizons drained away water amounting to 8.1, 6.2 and 3.1 mm, respectively. The drainage flux of 0.001 mm h^{-1} equivalent to DUL was realised after 660 h (28 days) after drainage for the A and B horizons while from the C horizon DUL was realised after 390 h (16 days). Corresponding SWC was 0.30 mm mm^{-1} for the A and B

horizons and 0.31 mm mm^{-1} for the *C* horizon. The student's *t*-test also confirmed the similarities observed between the upper horizons.

- Sepane: from the θ-T relationship of the three horizon layers soil water content increased with depth while drainage rates decreased. The amount of water that drained away from field saturation of 0.326, 0.332 and 0.338 mm mm^{-1} within the first 3 h was 4.7, 2.8 and 2 mm for the respective *A*, *B* and *C* horizons. At the end of 200 h the layers drained a respective water content amounting to 8.5, 5.4, and 3 mm. The drainage flux of 0.001 mm h^{-1} was attained after 660, 480 (20 days) and 300 (13 days) hours from saturation at SWC of 29.4, 31.7 and 32.3 mm mm^{-1}, for the *A*, *B* and *C* horizons, respectively. The student's *t*-test also confirmed the comparable differences found between these soil horizons.
- Swartland: soil water content was concentrated on the upper soil horizons with the *B* horizon assuming a higher water content regime throughout the drainage period. The amount of water that drained away within 3 h was 4.6 mm from the *A* horizon, 3.76 mm from the *B* horizon and 6 mm from the *C* horizon. After 200 h of drainage 8.6 mm, 7.5 mm and 26 mm drained from an initial field saturation of 0.34, 0.344 and 0.33 mm mm^{-1} for the *A*, *B* and *C* horizons, respectively. A drainage flux of 0.001 mm h^{-1} was achieved after 672 (28 days) hours from the *A* and *B* horizons with a respective SWC of 0.29 and 0.30 mm mm^{-1}. Although the student's *t*-test found these two horizons to be comparable the pooled variation was the least among the pairs.

3.5 Total drainage and flux rates

Total drainage and flux rates from the internal drainage trial were summarized in Table 9 and Fig. 7, respectively. The respective drainage amounts from the three soil types showed a decrease with depth with the exception in the Swartland. In all the soils the amount that drained away from approached negligible levels (DUL) at drainage flux rate of 0.001 mm h^{-1}. At this flux rate the total water loss was equivalent to 0.09 % of the 550 mm annual average rainfall of the area.

4 Discussion

The internal drainage property was consistent with the presence and intensity of layering from the Tukulu, Sepane and Swartland soils. Evidence of slight wind erosion in the absence of flooding or water erosion could suggest that eutrophic conditions of the semi arid environment played a critical role in the development of the layering pattern of these soils. Moderate physical and chemical weathering of underlying material of solid rock of binary origin affirm the in-situ evolution of the three soil types. Despite the similarities in parent rock material and orthic *A* horizons, the differences in subsurface layers could be explainedby the geological position each soil occupied in the landscape. The Tukulu and Swartland had a weakly developed *A* and *B* horizons with a smooth transition at the interface denoting a weak layering between these horizons. Chimungu (2009) treated the Tukulu upper horizons as homogenous in order to describe the internal drainage by the unity gradient approach recommended by Yeh et al. (1985). The clay rich underlying horizons found in the Tukulu and Sepane was indicative of the common drainage line shared by these soils and that these clayey horizons were of alluvial origin (Hensley, et al., 2006).

Given that internal drainage is accountable to gravitational flow boundary conditions, the hydraulic characteristics of the underlying soil profile layers are key this process (Blume et al., 2009; Chimungu, 2009; Nhlabatsi, 2010). Consistent with the restrictive clay layer of the prismacutic *C* horizons was 21 and 20 mm of water that drained away from the respective Tukulu and Sepane. Corresponding to the weakly developed Swartland was 51 mm from which 32 mm was contributions by the saprolite *C* horizon. This was not expected given the coarseness of the saprolite rock with K_s values of about 77 mm h^{-1}. Hensley et al. (2000) and Botha et al. (2003) concluded that the saprolite layer was ill-posed for deep soil water storage given its high water release characteristics. This was consistent with the illustrations given by Hillel (2004) about soils with an underlying course texture horizon havng a drier soil water regime. However, the pedocutanic *B* horizon when fully developed could have clay content exceeding 30 % that was acceptable for soil water conservation under IRWH technique (Hensley et al., 2000; Botha, et al., 2007).

Evidence of the slow drainage properties of the clay rich layer(s) in the Tukulu and Sepane was the presence of hydromorphic mottles confirming that soil water was subjected to restricted flow above these layer(s). In the Sepane hydromorphic mottles were also found at depths of 300 to 700 mm reflecting the effect of the pedocunatic clay rich *B* horizons on internal drainage. Nevertheless, the prismacutanic layers were the most restrictive with 9.6 and 1.9 $\mathrm{mm\,h^{-1}}$ from the Tukulu and Sepane, respectively. The latter realised a flux rate of 0.001 $\mathrm{mm\,h^{-1}}$ after 13 days of drainage while the former after 16 days. The same flux rate from the Tukulu was recorded after 26 days of drainage by Chimungu (2009). However, the more restriction on internal drainage of the Sepane could be explained by the duality of heavy structured layers in this profile (Fraenkel, 2008). Prospects of having a positive pressure head building up from the restrictive layers (Tartakovsky et al., 2003) does support the high drainage rate observed at the early hours of drainage from the Tukulu and Sepane. Inconsistencies in drainage amounts within each soil profile could reflect poor sealing of the monoliths side walls against lateral leakage, a scenario that was also a concern to Hopmans et al. (2002) and experienced by Chimungu (2009) on the same monoliths. Over and above, the *C* horizons from the Tukulu and Swartland controlled the permissible drainage from the upper horizons, a scenario that was confirmed by the fusion of the flux curves from these two soils. Greater spatiality from the Swartland flux curves suggested that the saprolite layer exhibited less control on how the upper horizons drained.

Considering the θ-h and K-θ relationships provided further evaluation of the presence of soil profile layers on the drainage process. Driven by gravitational potential drainage the process involves suction and K-coefficients of permeability near saturation (Schaap and van Genuchten, 2006; Scheffler, 2007). Corresponding drainage pore space are those of diameters ranging from 1000 µm to several mm (Luxmoore, 1981). The variation in these classes of pores was noticeable within the suction range of 300 to 1000 mm from the soil layers of the three soil profiles. However, the small volume of drainable pores (Dane and Hopmans, 2002; Schaap and van Genuchten, 2005) found on clay rich horizons was confirmed by the almost level or gentle slope of the θ-h relationship depicting a slow release. Deficiencies in clay and structure from the Swartland profile layers, especially the saprolite C horizon resulted to the steep θ-h relationship that was consistent with the high water release during the internal drainage. Intensity of layering among the three soils was also captured by the abrupt changes in K_s downwards the profile within suction ranging from -10 to -100 mm (Zavattaro and Grignani, 2001). Notable was the drop from 40 to 9.6 mm h^{-1} between the neocutanic B and prismatic C horizons for the Tukulu. This discontinuities were consistent with the the behaviour of flow and unpredictable nature of hydraulic properties in layered soils (Mathews et al., 2004). Another drop of 18.1 to 2 mm h^{-1} between the Sepane pedocutanic B and prismatic C horizons was recorded alongside the observation that increased clay content with depth restricted internal drainage (Romano et al., 1996; Bohne, 2005; Gopalakrishnan and Manik, 2007; Jones et al., 2009).

Variation in K-θ relationship was also able to show the decline in available water for drainage irrespective of SWC and depth. Distinguishable were the steep gradients of the K-θ relationships from the pedocutanic and prismatic horizons with corresponding hydraulic gradient fairly above unity. From the orthic and neocutanic horizons this gradient was almost equal to 1 suggesting that the adoption of the unity gradient by Chimungu (2009) in approximating the K-θ relationship of these horizons was reasonable. However, application of the unity gradient is questioned by most researchers especially on clay soils where the K-coefficient could drop by several orders of magnitude within a narrow range of SWC (Reichardt, 1993; Bacchi and Reichardt, 1993). Supporting this sentiment was the observation that the K-coefficient from the Tukulu and Sepane was less than drainage flux at DUL by order of one magnitude. The rapid fall of K-coefficient by several orders of magnitudes while SWC remained within the near saturation range was also acknowledged by Hensley et al. (2000) who related this function to the requirements of IRWH for deep soil water storage. However, the affinity to water shown by soils predominated by micro-pores of diameter less than 30 µm (Luxmoore, 1981), has raised questions on the availability of water tightly held against gravity, to roots of crop plants (Whitmore and Whalley, 2009). Nevertheless, it can be deduced from this work that the presence of soil layers and their respective permeability from the three soils affected drainage differently, and hence soil water storage.

5 Conclusions

The evaluation of soil layers on internal drainage from the Tukulu, Sepane and Swartland soil types earmarked for IRWH production technique was the main objective of the study. Integrating in-situ and laboratory desorption procedures provided the opportunity to reflect on the pedological presence of soil layers and also to relate their morphological features to the hydraulic characteristics that governed the drainage process.

Critical conclusions were drawn from the total and rate of drainage expressed by the three soil profiles. By virtue of their fine size (less than 0.002 mm) the clay fraction determined the extent of layering, both in texture and structure. Consequently, the clay content influenced the soil water release and permeability during drainage. Soil horizons with clay content ranging from 26 to 48 % contributed less than 5 mm to total drainage irrespective of textural and structural class. This suggests that from an annual rainfall of 550 mm drainage losses from each profile layer with clay content falling in this category should be around 1 % of the total rainfall. Considering drainage flux of 0.001 mm h^{-1} to correspond to DUL produced realistic estimates that were consistent with the slope of θ-T relationships and could be used to estimate DUL from other layered soils especially those earmarked for IRWH.

Proven by this work was the variation of drainage with the degree of soil layering. The coefficient of both saturation and de-saturation allowed reflection on the extent at which drainage was influenced by the presence of an abrupt or smooth transitional change in clay content and structure. Increased matrix suction against gravitational influence on clay rich profile layers had a significant influence in lowering the K-θ coefficient to negligible levels at relatively high soil water contents. This function was transferred to overlying layers irrespective of their textural and structural orientation suggesting the importance of clay soils on the overall permeability of the profile when occurring on the lower horizons in particular. About 1 % of the total annual rainfall was lost from the soil profile layers of the Tukulu and Sepane suggesting their greater potential for soil water conservation, especially for IRWH. Aspects of deep infiltration and runoff could become management issues when clay rich soil layers occur at shallow depths of 300 mm. On the contrary, the deficiency in layers rich in clay and structure from the Swartland proven by the deep drainage and drier soil water regime presented this soil as a lower potential for IRWH development.

Acknowledgements. We acknowledge the technical support rendered by the management and staff of Paradys experiment station. Gratitude's to Malcom Hensley for his contributions in classifying the opened soil profiles and assistance in setting up the hanging soil column method. Special thanks also to Liesl van der Westhuizen for her constructive suggestions on improving the writing of this manuscript.

References

Acutis, M. and Donatelli, M.: SOILPAR 2.00; Software to estimate soil hydrological parameters and functions, Eur. J. Agron., 18, 373–377, 2003.

Bacchi, O. O. S.: Comparative analysis of soil hydraulic conductivity methods for unsaturated soils. Piracicaba, Escola Superior de Agricultua Luiz de Queiroz, Tese de Doutorado, 94 pp., 1988.

Bacchi, O. O. S. and Reichrdt, K.: On simple methods for unsaturated soil hydraulic conductivity determination, Sci. Agric. Piracicaba, 50, 326–328, 1993.

Bennie, A. T. P.: Managing the profile available water capacity for irrigation of annual crops in arid regions, University of the Free State, Bloemfontein, South Africa, 1994.

Bittelli, M. and Flury, M.: Errors in water retention curves determined with pressure plates, SSAJ, 73, 1453–1460, 2009.

Bohne, K.: An Introduction into Applied Soil Hydrology, Catena Verlag GmbH, Reiskirchen, Germany, 2005.

Botha, J. J., van Rensburg, L. D., Anderson, J. J., Hensely, M., Macheli, M. S., van Staden, P. P., Kundhlande, G., Groenewald, D. G., and Baiphethi, M. N.: Water conservation techniques on small plots in semi-arid areas to enhance rainfall use efficiency, food security, and sustainable crop production, Water Research Commission, Report 1176/1/03, Pretoria, South Africa, p.27, 2003.

Botha, J. J., Anderson, J. J., Groenewald, D. C., Mdibe, N., Baiphethi, M. N., Nhlabatsi, N. N., and Zere, T. B.: On-farm application of In-field rainwater harvesting techniques on small plots in the central region of South Africa, Water Research Commission, Report, TT 313/07, Pretoria, South Africa, 2007.

Blume, T., Zehe, E., and Bronstert, A.: Use of soil moisture dynamics and patterns at different spatio-temporal scales for the investigation of subsurface flow processes, Hydrol. Earth Syst. Sci., 13, 1215–1233, doi:10.5194/hess-13-1215-2009, 2009.

Chimungu, J. G.: Comparison of field and laboratory measured hydraulic properties of selected diagnostic soil horizons, M.Sc. (Agric) Dissertation, University of the Free State, Bloemfontein, South Africa, 2009.

Dane, J. H. and Hopmans, J. W.: Soil water retention and storage – introduction, in: Methods of Soil Analysis, Part 4, Physical Methods, edited by: Dane, J. H. and Topp, G. C., Soil Science Society of America Book Series No. 5, 671–674, 2002.

Dane, J. H. and Hruska, S: In-situ determination of soil hydraulic properties during drainage, Soil Sci. Soc. Am. J., 47, 619–624, 1983.

Dirksen, C.: Soil Physical Measurements. Geo-Ecology Paperback, Catena Verlag GmbH, Reiskirchen, 1999.

Eching, S. O. and Hopmans, J. W.: Optimization of hydraulic functions from transient outflow and soil water pressure data, Soil Sci. Soc. Am., 57, 1167–1175, 1993.

Eching, S. O., Hopmans, J. W., and Wendroth, O.: Unsaturated hydraulic conductivity from transient multistep outflow and soil water pressure data, Soil Sci. Soc. Am. J., 58, 687–695, 1994.

FAO: Bio-Physical requirements and socio-economic acceptance of infield rainwater harvesting and conservation in the semi-arid central region of South Africa, available at: http://www.fao.org, last access: 20 October 2009.

Fraenkel, C. H.: Spatial variability of selected soil properties in and between map units, M.Sc. (Agric) Dissertation, University of the Free State, Bloemfontein, South Africa, 2008.

Gomez, K. A. and Gomez, A. A,: Statistical Procedures for Agricultural Research, 2nd Edn., John Wiley and Sons, New York, 1984.

Gopalakrishnan, K. and Manik, A.: A mathematical model for predicting isothermal soil moisture profiles using finite different methods, Int. J. Comput. Math. Sci., 1, 128–134, 2007.

Hensley, M., Botha, J. J., Anderson, J. J., Van Staden, P. P., and Du Toit, A.: Optimising rainfall use efficiency for developing farmers with limited access to irrigation water. Water Research Commission report 878/1/00, Pretoria, South Africa, 2000.

Hensley, M., Le Roux, P. A. L., Du Preez, C. C., Van Huyssteen, C., Kotze, E., and Van Rensburg, L. D.: Soils; the free state agricultural base, S. Afr. Geogr. J., 88, 11–21, 2006.

Hillel, D., Krentos, V. D., and Styllianou, Y.: Procedure and test of an internal drainage method for measuring soil hydraulic characteristics in situ, Soil Sci., 114, 395–400, 1972.

Hillel, D. H.: Environmental Soil Physics, Academic Press, New York, 2004.

Hurtado, A. L. B., Cichota, R., and Jong van lier, Q.: Parametrização do método do perfil instantâneo para a determinação da condutividade hidráulica do solo em experimentos com evaporação, R. Bras. Ci. Solo, 29, 301–307, 2005.

Jones, E. W., Koh, Y. H., Tiver, B. J., and Wong, M. A. H.: Modelling the behaviour of unsaturated, saline clay for geotechnical design, School of Civil, Environmental and Mining Engineering, University of Adelaide, 2009.

Jury, W., Gardener, W. R., and Gardner, W. H.: Soil Physics, 5th Edn., John Wiley and Sons, New York, 1991.

Kool, J. B., Parker, J. C., and van Genuchten, M. T.: determining soil hydraulic properties from one step outflow experiments by parameter estimation: theory and numerical studies, Soil Sci. Soc. Am. J., 49, 1348–1354, 1985.

Leij, F. J., Alves, W. J., and van Genuchten, M. T.: UNSODA: The Unsaturated Soil Hydraulic Database, US Salinity Lab., Riverside, CA, 1996.

Libardi, P. L., Reichardt, K., Nielsen, D. R., and Biggar, J. W.: Simple field methods for estimating soil hydraulic conductivity, Soil Sci. Soc. Am. J., 44, 3–7, 1980.

Luxmoore, R.: Micro-, Meso- and macroporosity of soil, Soil Sci. Soc. Am. J., 45, 241–285, 1981.

Mathews, C. J., Knight, F. J., and Braddock, R. D.: Using analytic solutions for homogeneous soils to assess numerical solutions for layered soils. ARC Discovery Indigenous Research Development Program, 31 April 2011, 2004.

Neto, D. D., Reichardt, K., Lúcia da Silva, A., Bacchi, O. O. S., Timm, L. C., Oliveira, J. C. M., and Nielsen, D. R.: A software to calculate soil hydraulic conductivity in internal drainage experiments (SHC, version 2), R. Bras. Ci. Solo, 31, 1219–1222, 2007.

Nielsen, D. R., Davison, J. M., Biggar, J. W., and Miller, R. J.: Water movement through Panoche clay loam soil, Hilgardia, 35, 491–506, 1964.

Non Affiliated Soil Analysis Work Committee: Handbook of Standard Soil Testing Methods for Advisory Purposes, Soil Science Society of South Africa, Pretoria, 1990.

Nhlabatsi, N. N.: Soil water evaporation studies on the Glen/Boheim ecotope, Ph. D. Thesis, University of the Free State, Bloemfontein, South Africa, 2011.

Ratliff, L. F., Richie, J. T., and Cassel, D. K.: Field measured limits of soil water availability as related to laboratory-measured properties, Soil Sci. Soc. Am. J., 47, 770–775, 1983.

Reichardt, K.: Unit gradient in internal drainage experiments for the determination of soil hydraulic conductivity, Sci. Agr. Piracicaba., 50, 151–153, 1993.

Reichardt, K., Timm, L. C., Bacchi, O. O. S., Oliveira, J. C. M., and Dourado-neto, D.: A parameterized equation to estimate soil hydraulic conductivity in the field, Aust. J. Soil Res., 42, 283–287, 2004.

Richards, L. A., Gardener, W. R., and Ogata, G.: Physical processes determining water loss from soil, Soil Sci. Soc. Am. Proc., 20, 310–314, 1956.

Romano, N., Brunone, B., and Santini, A.: Numerical analysis of one-dimensional unsaturated flow in layered soils, Adv. Water Res., 21, 315–324, 1996.

Rose, C. W., Stern, W. R., and Drummond, J. E.: Determination of hydraulic conductivity as a function of depth and water content for soil in situ, Aust. J. Soil Res., 3, 1–9, 1965.

Schaap, M. G. and van Genuchten, M. T.: A modified Mualem-van Genuchten formulation for improved description of the hydraulic conductivity near saturation, Vadose Zone J., 5, 27–34, 2006.

Scheffler, G.: Determination of instantaneous moisture content and moisture potential profiles, University of Technology, Dresden, 2007.

Title Page
Abstract | Introduction
Conclusions | References
Tables | Figures
◀▮ | ▶▮
◀ | ▶
Back | Close
Full Screen / Esc
Printer-friendly Version
Interactive Discussion

Scotter, D. R., Clothier, B. E., and Harper, E. R.: Measuring saturated hydraulic conductivity and sorptivity using twin rings, Aust. J. Soil Res., 20, 295–304, 1982.

Simunek, J., Wendroth, O., and van Genuchten, M. T.: Estimating unsaturated soil hydraulic properties from laboratory tension disc infiltrometer experiments, Water Resour. Res., 35, 2965–2979, 1999.

Slawinski, C., Witkowska-Walczak, B., and Walczak, R. T.: Determination of Water Conductivity Coefficient of Soil Porous Media, Institute of Agrophysics PAS, Lublin, 2004.

Soil Classification Working Group: Soil Classification – A Taxonomic System for South Africa. Memoirs on the Agricultural Natural Resources of South Africa Nr. 15, Department of Agricultural Development, Pretoria, 1991.

Tartakovsky, D. M., Lu, Z., Guadagnini, A., Tartakovsky, A. M.: Unsaturated flow in heterogeneous soils with spatially distributed uncertain hydraulic parameters, J. Hydrol., 275, 182–193, 2003.

The non-affiliated soil analysis work committee: Handbook of Standard Soil Testing Methods for Advisory Purposes, SSSSA, Pretoria, 1990.

Vachaud, G. and Dane, J. H.: Instantaneous profile, in: Methods of Soil Analysis, Part 4, Physical Methods, edited by: Dane, J. H. and Topp, G. C., SSSA Book Series 5, Madison, WI, 937–945, 2002.

Vachaud, G. C. Donko, D. S., and Thony, J. L.: Methodes decaracterisation hydrodynamique in situ dun sol non sature. Aplication a deux types de sol du Senegal en vue de la determination des termes du bilan hydrique, Ann. Agron., 29, 1–36, 1978.

van Dam, J. C., Stricker, J. N. M., and Droogers, P.: Inverse method to determine soil hydraulic functions from multistep outflow experiments, Soil Sci. Soc. Am. J., 58, 647–652, 1994.

Villagra, M. M., Michiels, P., Hartmann, R., Bacchi, O. O. S., and Reichardt, K.: Field determined variation of the unsaturated hydraulic conductivity functions using simplified analysis of internal drainage experiments, Sci. Agr. Piracicaba, 51, 113–122, 1994.

Vomicil, J. A.: Porosity, in: Methods of Soil Analysis, Part 1, edited by: Black, C. A., Am. Soc. Agron., Madison, 299–314, 1965.

Waston, K. K.: An instantaneous profile method for determining the hydraulic conductivity of unsaturated porous materials, Water Resour. Res., 2, 709–715, 1966.

Whitmore, A. P. and Whalley, W. R.: Physical effects of soil drying on roots and crop growth, J. Exp. Bot., 60, 2845–2857, 2009.

Wildenschild, D., Hopmans, J. W., and Simunek, J.: Flow rate dependence of soil hydraulic characteristics, Soil Sci. Soc. Am. J., 65, 35–48, 2001.

Yeh, T. C. J., Gelhar, L. W., and Gutjahr, A. L.: Stochastic analysis of unsaturated flow in heterogeneous soils, 2, Statistically anisotropic media with variable *a*, Water Resour. Res., 21, 457–464, 1985.

Zavattaro, L. and Grignani, C.: Deriving hydrological parameters for modelling water flow under field conditions, Soil Sci. Soc. Am. J., 65, 655–667, 2001.

Table 1. Summary of the physical and chemical characteristics of the three soil types.

Soil physical properties									
Soil forms	Tukulu			Sepane			Swartland		
Master Horizons	*A*	*B*1	*C*	*A*	*B*1	*C*	*A*	*B*1	*C*
Coarse sand (%)	5.3	9.2	2.1	5.2	3.5	2.3	4.7	3.2	54.3
Medium sand (%)	9.3	8.8	3.8	10	4.1	2.3	7.6	5.3	4.6
Fine sand (%)	41.2	31	28.3	41.9	41	31	42	37.6	17.2
Very fine sand (%)	25.3	21	8.4	21.5	10.5	18	31.7	26.6	2.5
Coarse silt (%)	2.1	2	3	1	3	1	2	3	3
Fine silt (%)	4.6	2.5	6.5	1	3	1	1	2	3
Clay (%)	11.3	26.4	47.9	19	35	45	11.3	21.9	15
Bulk density (kg m^{-3})	1670	1597	1602	1670	1790	1730	1670	1530	1450
Porosity (%)	34.0	33	32.4	34	33.5	33.8	35	39.9	41.6
K_s (mm h^{-1})	36.1	40	9.6	35.2	18.1	1.9	23.5	42.8	76.5
Chemical properties									
pH (water)	5.8	6.1	6.5	5.9	6.2	6.3	5.5	5.8	6.8
Ca ($\text{c mol}_c\ \text{kg}^{-1}$)	35.3	40.8	62.7	30.53	46	50	23	25.78	45
Mg ($\text{c mol}_c\ \text{kg}^{-1}$)	18.8	20.8	54.7	13.89	21.87	29.76	12.1	13.1	25.4
K ($\text{c mol}_c\ \text{kg}^{-1}$)	12.8	6.8	12.9	4.63	8.21	7.05	5.5	7.45	7.7
Na ($\text{c mol}_c\ \text{kg}^{-1}$)	2.4	2.5	3.4	1.96	3.8	3.91	0.7	1.52	2.3

K_s = saturated hydraulic conductivity.

Table 2. θ-h regression functions of soils horizons for the 0–1000 mm suction range.

Soil type	Horizons	Regression	R^2
Tukulu	*A*	$\theta = 0.332–0.00005\,\mathrm{h}$	0.98
	B	$\theta = 0.328–0.00004\,\mathrm{h}$	0.96
	C	$\theta = 0.324–0.000003\,\mathrm{h}$	0.93
Sepane	*A*	$\theta = 0.327–0.00007\,\mathrm{h}$	0.99
	B	$\theta = 0.333–0.00004\,\mathrm{h}$	0.99
	C	$\theta = 0.338–0.00004\,\mathrm{h}$	0.99
Swartland	*A*	$\theta = 0.339–0.00008\,\mathrm{h}$	0.99
	B	$\theta = 0.347–0.00006\,\mathrm{h}$	0.99
	C	$\theta = 0.345–0.00013\,\mathrm{h}$	0.97

Title Page
Abstract Introduction
Conclusions References
Tables Figures
◀I ▶I
◀ ▶
Back Close
Full Screen / Esc
Printer-friendly Version
Interactive Discussion

Table 3. Student's t-test for differences between horizons θ-h regression coefficients.

Soil type	Horizons	Pooled variance	Tabulated variance (α; 0.05)
Tukulu	*AB*	3.002	2.145
	BC	12.295	2.145
	AC	18.688	2.145
Sepane	*AB*	13.868	2.145
	BC	2.776	2.145
	AC	16.516	2.145
Swartland	*AB*	5.819	2.145
	BC	8.489	2.145
	AC	5.541	2.145

Table 4. K-θ relationships linear regression functions for the three soil types.

Soil type	Horizon	Regression	R^2
Tukulu	A	$\log K = 186.1(\theta) - 58.42$	0.94
	B	$\log K = 167.4(\theta) - 52.24$	0.99
	C	$\log K = 274.1(\theta) - 87.82$	0.97
Sepane	A	$\log K = 143.9(\theta) - 45.21$	0.99
	B	$\log K = 281.3(\theta) - 91.58$	0.98
	C	$\log K = 260.4(\theta) - 86.51$	0.87
Swartland	A	$\log K = 124.3(\theta) - 39.64$	0.89
	B	$\log K = 120.6(\theta) - 39.15$	0.97
	C	$\log K = 43.29(\theta) - 12.62$	0.99

Table 5. Homogeneity test for the three soils horizons.

Soil types	Bartletts test Computed $\chi 2$	 Tabular $\chi 2$ $(\alpha; 0.05, 2)$	Regression coefficient Computed F $(\alpha; 0.05, 2)$	 Tabular F $(\alpha; 0.05, 2)$
Tukulu	19.36	5.99	27.71	3.16
Sepane	26.75	5.99	51.99	3.16
Swartland	32.46	5.99	119.29	3.16

Table 6. Student's t-test for differences between horizons K-θ regression coefficients.

Soil type	Horizons	Pooled variance	Tabulated variance (α; 0.05)
Tukulu	*AB*	1.714^{ns}	2.032
	BC	9.905	2.032
	AC	5.092	2.032
Sepane	*AB*	14.558	2.032
	BC	0.841^{ns}	2.032
	AC	6.121	2.032
Swartland	*AB*	0.336^{ns}	2.032
	BC	18.584	2.032
	AC	10.729	2.032

ns = not significantly different at 95 % confidence interval.

Table 7. θ-T relationships linear regression functions for the three soil types.

Soil form	Horizons	Regression	R^2
Tukulu	*A*	$y = 0.317x^{-0.009}$	0.96
	B	$y = 0.319x^{-0.009}$	0.99
	C	$y = 0.320x^{-0.005}$	0.99
Sepane	*A*	$y = 0.316x^{-0.011}$	0.99
	B	$y = 0.328x^{-0.005}$	0.99
	C	$y = 0.332x^{-0.005}$	0.97
Swartland	*A*	$y = 0.318x^{-0.013}$	0.92
	B	$y = 0.328x^{-0.013}$	0.97
	C	$y = 0.308x^{-0.045}$	0.99

Table 8. Student's t-test for the differences between horizons θ-T regression coefficients.

Soil type	Horizons	Pooled variance	Tabulated variance (α; 0.05)
Tukulu	*AB*	1.153^{ns}	2.032
	BC	12.977	2.032
	AC	4.145	2.032
Sepane	*AB*	5.178	2.032
	BC	6.977	2.032
	AC	7.854	2.032
Swartland	*AB*	3.247	2.032
	BC	44.447	2.032
	AC	13.161	2.032

Table 9. Amount of soil water that drained away from horizons.

		Accumulative water depth (mm) at different drainage periods (h)								
Soil type	Horizons	18	24	72	210	300	390	660	930	1200
Tukulu	*A*	6.44	6.63	7.38	8.09	8.33	8.51	8.86	9.08	9.25
	B	3.94	4.21	5.23	6.21	6.54	6.78	7.25	7.56	7.79
	C	2.15	2.26	2.69	3.11	3.25	3.35	3.56	3.69	3.79
Sepane	*A*	6.38	6.64	7.62	8.56	8.87	9.10	9.55	9.84	10.06
	B	3.88	4.06	4.77	5.45	5.68	5.84	6.18	6.39	6.56
	C	2.36	2.43	2.72	3.00	3.09	3.16	3.29	3.38	3.45
Swartland	*A*	7.40	7.55	8.15	8.70	8.89	9.04	9.34	9.51	9.65
	B	5.42	5.67	6.64	7.52	7.83	8.08	8.55	8.83	9.04
	C	16.70	17.87	22.21	26.03	27.35	28.37	30.32	31.45	32.29

Table A1. Profile description of the Tukulu form soil.

Map/photo:	2926 Bloemfontein	Soil form and Family:	Tukulu Dikeni
Latitude + Longitude:	29°13′25′′/26°12′′	Surface rockiness:	None
Altitude:	1421.9 m	Occurrence of flooding:	None
Terrain unit:	Midslope	Wind erosion:	Slight wind
Slope:	1 %	Water erosion:	None
Slope shape:	Straight	Vegetation/land use:	Agronomic field crops
Aspect:	South	Water table:	None
Micro relief:	None	Described by:	M. Hensley/S. Mavimbela
Parent material Solum:	Origin binary, aeolin, solid rock	Date described:	1 Nov 2006
Underlying material:	Sandstone (Feldspathic)	Weathering of underlying material:	Moderate physical, moderate chemical
		Alternation of underlying material:	Ferrugised

Horizon	Depth (mm)	Description	Diagnostic horizon
A	0–300	Moist state; dry colour: reddish brown (5YR4/8); moist colour; reddish brown (5YR4/8); texture: fine sandy loam; structure: apedal massive: consistence: friable; few fine pores; common roots; gradual transition	Orthic
*B*1	300–600	Moist state; dry colour: reddish brown (5YR3/6); reddish brown (5YR3/6); texture: fine sandy clay loam; Neocutanic Structure: apedal massive becoming weak subangular blocky towards transition: consistence: friable; few fine pores; few clay cutans; very few fine pores; common roots; clear, tonguing transition	Neoucutanic
*C*1	600–850	Moists state; dry colour. Dark grey, olive and yellow mottles; moist colour: olive grey with yellow mottles; texture: clay; common distinct grey material, and yellow reduced iron oxide mottles; few prominent black oxidised iron oxide mottles; structure: prismatic; consistence firm; few slickensides; common clay cutans; very few roots; gradual transition	Unconsolidated with signs of wetness
*C*2	850–±1350	Allows water to enter, hence the presence roots. It chops out the profile relatively easily up to ±1350 m, getting harder towards the bottom and probably very impermeable slightly deeper. Unconsolidated:	Soft rock

Title Page
Abstract | Introduction
Conclusions | References
Tables | Figures
◀| |▶
◀ ▶
Back | Close
Full Screen / Esc

Printer-friendly Version

Interactive Discussion

Table A2. Profile description of the Sepane form soil.

Map/photo:	2926 Bloemfontein	Soil form and Family:	Sepane Rambles
		Surface rockiness:	None
Altitude:	1414.3 m	Occurrence of flooding:	None
Terrain unit:	Midslope	Wind erosion:	Slight wind
Slope:	1 %	Water erosion:	None
Slope shape:	Straight	Vegetation/land use:	Agronomic field crops
Aspect:	South	Water table:	None
Micro relief:	None	Described by:	M. Hensley/S. Mavimbela
Parent material Solum:	Origin binary, aeolin, solid rock	Date described:	1 Nov 2006
Underlying material:	Sandstone (Feldspathic)	Weathering of underlying material:	Moderate physical, moderate chemical
		Alternation of underlying material:	Ferrugised

Horizon	Depth (mm)	Description	Diagnostic horizon
A	0–300	Moist state; dry colour: reddish brown (5YR4/8); moist colour; reddish brown (5YR4/8); texture: fine sandy loam; structure: apedal massive: consistence: friable; few fine pores; common roots; abrupt transition	Orthic
*B*1	300–700	Moist state; dry colour: dark grey (5YR3/4); reddish brown (2.5YR3/4); texture: fine sandy clay loam; Pedocutanic Structure: moderate to medium sub-angular blocky: consistence: slightly firm; few normal fine pores; many clay cutans; clay Skins; common roots; abrupt transition	Pedocunatic
*C*1	700–800	Moists state; dry colour. Dark greyish brown (2.5YR4/2); moist colour: grey (2.5T5/0); texture: sandy clay; common distinct grey, and yellow reduced iron oxide mottles; abundance of red, grey and black mottles; structure: prismatic; consistence: slightly firm; few slickenside's; common clay cutans; very few roots; abrupt transition.	Prismacunatic
*C*2	800–±1000	Undisturbed, signs of calcium deposits, It chops out the profile relatively easily up to ±1350 m, getting harder towards the bottom and probably very impermeable slightly deeper. Unconsolidated:	Soft rock

Table A3. Profile description of the Swartland form soil.

Map/photo:	2926 Bloemfontein	Soil form and Family:	Swartland/Rouxville
		Surface rockiness:	None
Altitude:	1421.9 m	Occurrence of flooding:	None
Terrain unit:	Midslope	Wind erosion:	Slight wind
Slope:	1 %	Water erosion:	None
Slope shape:	Straight	Vegetation/land use:	Agronomic field crops
Aspect:	South	Water table:	None
Micro relief:	None	Described by:	M. Hensley/S. Mavimbela
Parent material Solum:	Origin binary, aeolin, local colluvium	Date described:	1 Nov 2006
Underlying material:	Sandstone (Feldspathic)	Weathering of underlying material:	Moderate physical, moderate chemical
		Alternation of underlying material:	Ferrugised

Horizon	Depth (mm)	Description	Diagnostic horizon
A	0–200	Moist state; dry colour: reddish brown (5YR5/8); moist colour; reddish brown (5YR/8); texture: fine sandy loam; structure: apedal massive: consistence: friable; few fine pores; common roots; clear smooth transition	Orthic
*B*1	200–400	Moist state; dry colour: dark reddish brown (5YR3/6); reddish brown (5YR3/6);texture: fine sandy clay; Pedocutanic Structure: moderate coarse sub-angular blocky: consistence: friable; very few fine sesquioxide concretions; few roots; smooth transition	Pedocunatic
*C*1	400 ± 700	Moist state; undisturbed; dolorite rock; black concretions; many reddish-yellow geogenic mottles, very few fine sesquioxides concretions; Non hardened free lime; strong effervescence, very few roots; not observed transition.	Saprolite

Title Page

Abstract | Introduction

Conclusions | References

Tables | Figures

◂◂ | ▸▸

◂ | ▸

Back | Close

Full Screen / Esc

Printer-friendly Version

Interactive Discussion

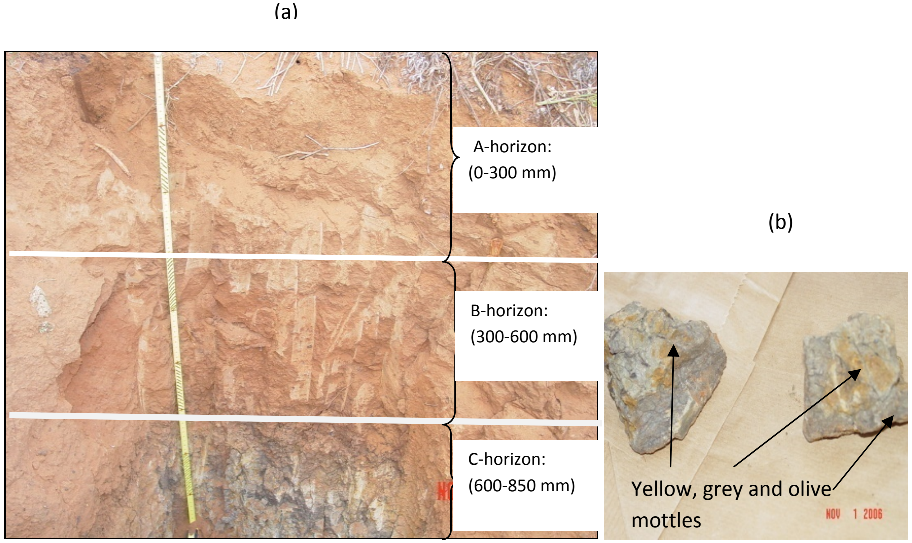

Fig. 1. Representative of the three opened profile pits from the Tukulu soil **(a)** and hydromorphic mottles present in the prismacutanic *C* horizon **(b)**.

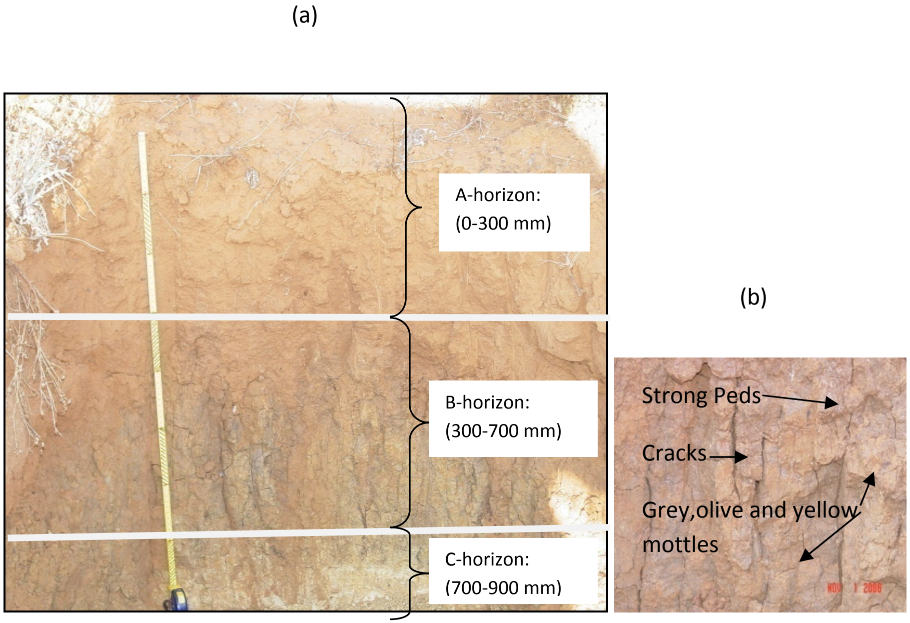

Fig. 2. Representative of the three opened profile pits from the Sepane soil **(a)** and strong peds with cracks and grey, olive and yellow mottles of the pedocutanic *B* horizon horizon **(b)**.

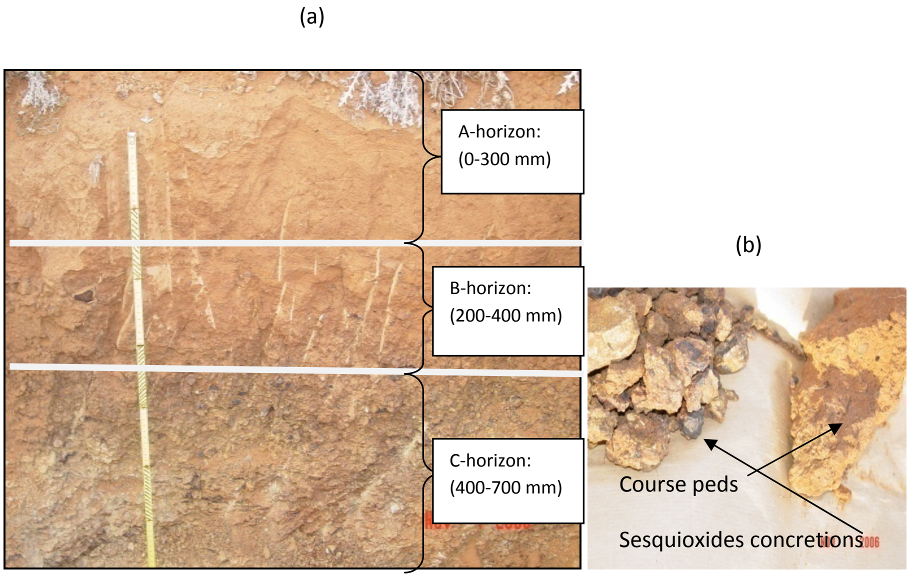

Fig. 3. Representative of the three opened profile pits from the Swartland soil **(a)** and course peds with Sesquioxides concretions in the pedocutanic *B* horizon **(b)**.

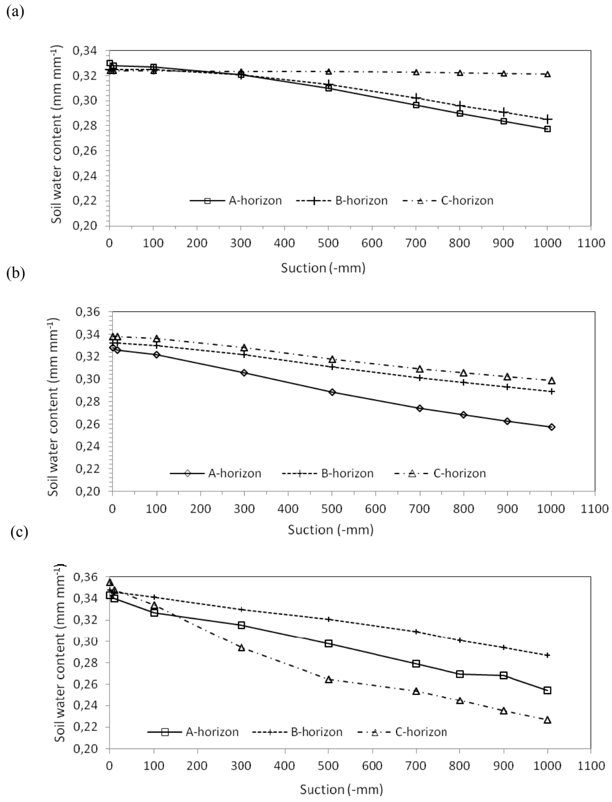

Fig. 4. θ-h relationships representing the soil water characteristics curve from 0 to −1000 mm suctions measured using the hanging soil column method from undisturbed core soil samples of the Tukulu **(a)**, Sepane **(b)** and Swartland **(c)** soil horizons.

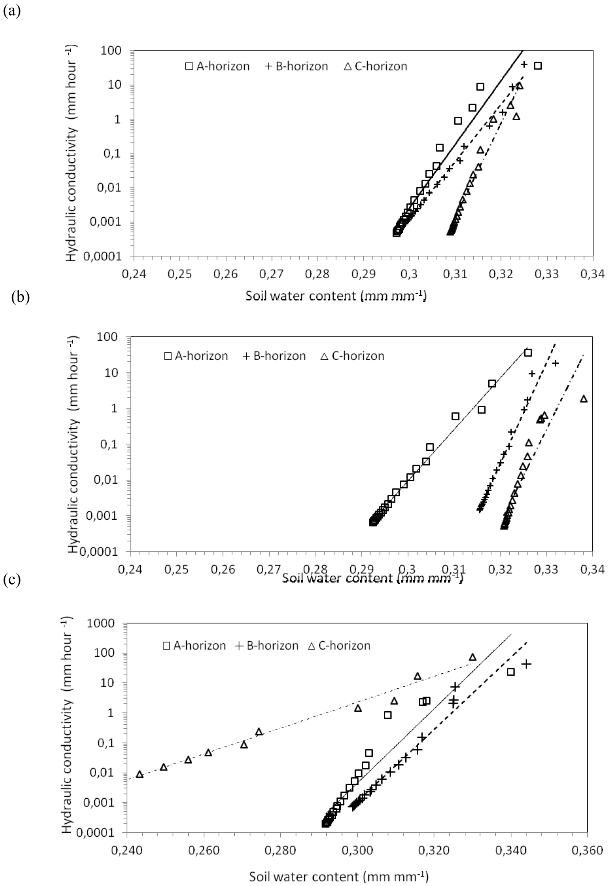

Fig. 5. K-θ-relationship representing variation in permeability during the 1200 h internal drainage period from saturation for the Tukulu, **(a)** Sepane **(b)** and Swartland **(c)** soil types.

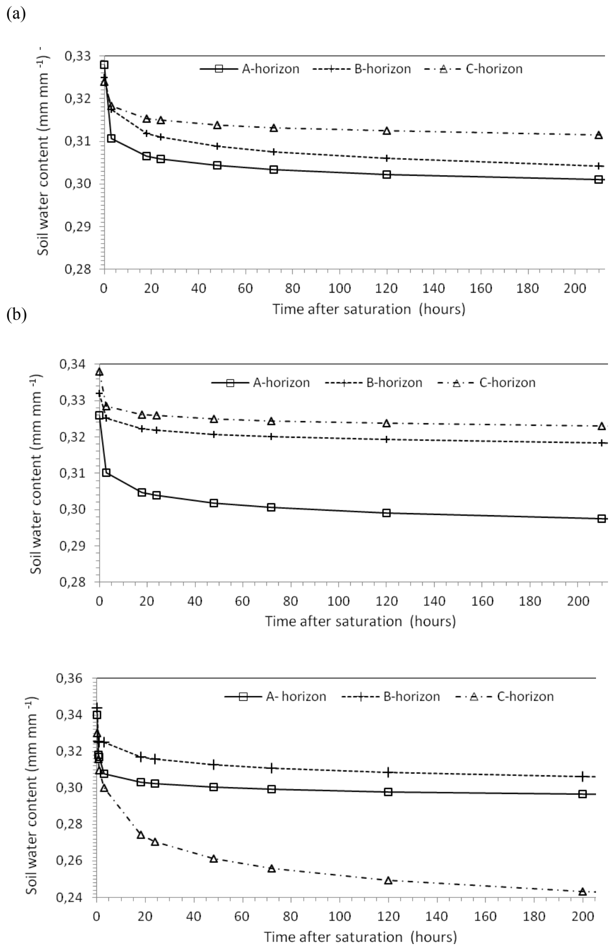

Fig. 6. θ-T relationships depicting the drainage curve during the first 200 h of drainage from saturation for the **(a)** Tukulu, **(b)** Sepane and **(c)** Swartland soil types

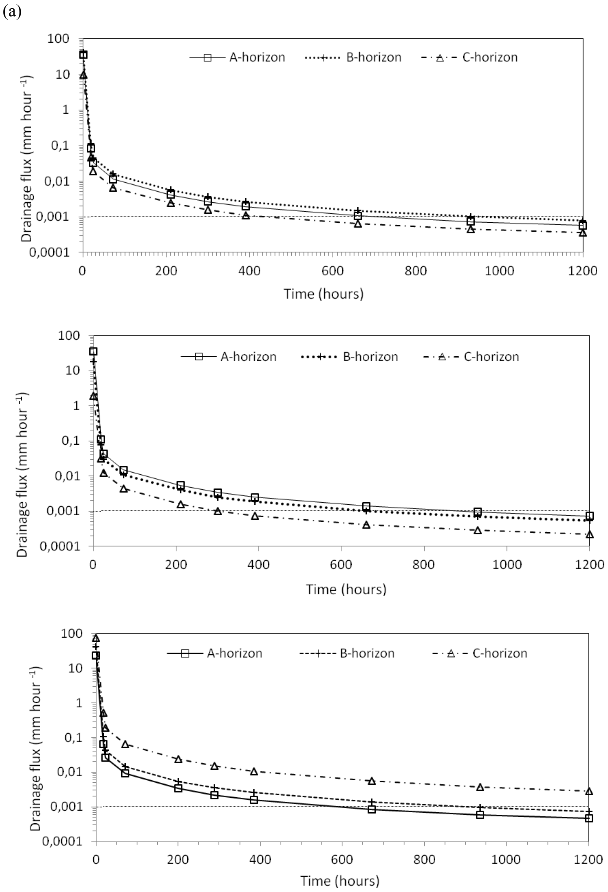

Fig. 7. Drainage flux from the Tukulu **(a)**, Sepane **(b)** and Swartland **(c)** soil profile horizons. Horizontal line cutting the drainage flux axis at 0.001 mm h^{-1} depicting the drainage upper limit flux rate after which increase in drainage period brings insignificant changes in soil water content.